J. Fluid Mech. (1965), *vol.* 21, *part* 4, *pp.* 659–672
Printed in Great Britain

Theory of heat transfer to a shock-tube end-wall from an ionized monatomic gas

By JAMES A. FAY
Massachusetts Institute of Technology, Cambridge, Massachusetts
AND NELSON H. KEMP
Avco-Everett Research Laboratory, Everett, Massachusetts

(Received 6 July 1964)

This paper deals with the calculation of the convective heat transfer rate to the end-wall of a shock tube from a monatomic gas heated by a reflected shock. We consider a range of shock strengths for which the equilibrium thermodynamic state is one of appreciable ionization. The resulting boundary-layer problem involves the thermal conductivity and ambipolar diffusion coefficient for a partially ionized monatomic gas. The formulation here is restricted to the case of a catalytic wall and equal temperatures for all species. We ignore the effect of the plasma sheath at the wall. Consideration is given to three limiting cases for which similarity-type solutions of the boundary-layer equations may be found: (1) complete thermodynamic equilibrium behind the reflected shock and within the boundary layer; (2) equilibrium behind the reflected shock, but no gas-phase recombination in the boundary layer; (3) no ionization in either region. Numerical calculations are carried out for argon using estimated values of thermal conductivity and ambipolar diffusion, and compared with shock-tube experiments of Camac & Feinberg (1965). For no ionization, calculations were made with thermal conductivity varying as the $\frac{3}{4}$ power of the temperature, which fits the estimates of Amdur & Mason (1958) up to 15,000 °K. Excellent agreement with experiment is obtained confirming an extrapolation of this power law up to 75,000 °K. For ionized cases, based on estimates of Fay (1964), the theory predicts heating rates 20–40 % lower than measured values. Some possible reasons for this discrepancy are discussed.

1. Introduction

The shock tube has been developed into a reliable apparatus for the production and study of high-temperature gases and plasmas. One frequently used experiment is the study of the gas left behind when the reflected shock wave recedes from the end of the shock tube. This gas is approximately uniform and quiescent, the only non-uniformities and motions being caused by 'viscous' effects, i.e. effects caused by the presence of cold walls surrounding the hot gas. Its equilibrium thermodynamic state is predictable from observations of the speeds of the incident and reflected shocks.† It is easily studied through the walls without

† The work of Camac & Teare (1964) indicates that for chemically reacting gases, the non-equilibrium thermodynamic state is not so easy to predict.

disturbing the bulk of the gas sample. Therefore, the method is conducive to determining the properties of gases, provided these properties can be related to observations made at the wall.

In this report we will relate the thermodynamic and transport properties of an ionized monatomic gas to the heat transfer measured at the end wall of the shock tube, provided only that the gas in the boundary layer is either frozen or at equilibrium. In other words, we will formulate and solve (for the case of argon) the boundary-layer heat-transfer problem for such a gas in the geometry in which a semi-infinite hot gas sample is suddenly put in contact with a plane, infinite, cold wall. This may be called the thermal Rayleigh problem, in analogy with the viscous Rayleigh problem in which a semi-infinite fluid is suddenly put in contact with a plane, infinite wall moving parallel to itself.

The geometry studied here has been previously utilized for studying thermal conductivity in unionized argon by Smiley (1957) and Lauver (1964), and in dissociated air by Hansen, Early, Alzofon & Wittenborn (1959), Peng & Ahyte (1961) and Thomson (1960). The upper temperature limit of Smiley's work was 3000 °K and that of Lauver 9000 °K. The formulations of Hansen *et al.* and Peng & Ahyte were incorrect because they ignored the convection toward the wall induced by the cooling of the gas at the wall. Thomson pointed out and corrected this error. Theoretical calculations applicable to unionized argon in the present geometry have been made by Edwards & Tellep (1961) and by Jepson (1961) in their studies of flow at zero Prandtl number of fluids with power law thermal properties. In the present study a remarkably accurate approximate formula due to Jepson is used to calculate the unionized heat-transfer.

The present study was motivated by experiments of Camac & Feinberg (1965), where heat transfer was measured from unionized argon up to 75,000 °K, and also from argon up to 45 % ionized. The theory and calculations reported here were performed to make it possible to compare the predicted heat-transfer rates based on present knowledge of the transport properties of argon with experimental observations.

In the succeeding sections we give the boundary-layer equations, the thermodynamic and transport properties, and the mathematical transformation used to make the calculations. Then we discuss the results compared to experimentally measured heat-transfer rates.

2. Boundary-layer equations

A simple boundary layer is envisaged, in which all species are taken to have the same temperature T. Only three cases are considered: (1) a perfect unionized monatomic gas; (2) an ionized gas in thermal equilibrium; (3) an ionized gas with an equilibrium free stream and a frozen (no gas-phase recombination) boundary layer. All these cases permit similarity solutions of the boundary-layer equations.

We imagine the cold end-wall of the shock tube suddenly put into contact at $t = 0$ with the quiescent hot gas. We assume the gas and the wall to be semi-infinite in extent so there is no flow parallel to the wall and no change in that

direction. All flow that ensues is in the direction normal to the wall, with mass velocity v and diffusion velocity V_i for the ith species. Changes occur only with time t and normal distance y.

When the usual boundary-layer simplifications are applied to the Navier–Stokes equations for this geometry, the tangential momentum equation is absent, and the normal momentum equation yields the familiar condition of constant pressure, $p = p_e$, the pressure at the external edge of the boundary layer, i.e. in the undisturbed plasma. The over-all mass conservation for mixture density ρ and normal velocity v requires

$$\frac{\partial \rho}{\partial t} + \frac{\partial \rho v}{\partial y} = 0, \tag{2.1}$$

while conservation of mass for the ith species relates its mass density ρ_i, its diffusion velocity V_i, and its mass rate of production per unit volume w_i by

$$\frac{\partial \rho_i}{\partial t} + \frac{\partial}{\partial y} \rho_i (v + V_i) = w_i. \tag{2.2}$$

The thermal-energy conservation is written in terms of the enthalpy h of the mixture as

$$\rho \frac{\partial h}{\partial t} + \rho v \frac{\partial h}{\partial y} = \frac{\partial}{\partial y}(-q_y), \tag{2.3}$$

where the left side is the convection of enthalpy, and q_y is the flux of energy normal to the wall. The latter has the form

$$q_y = -k \frac{\partial T}{\partial y} + \Sigma \rho_i V_i h_i, \tag{2.4}$$

where the first term is the Fourier heat-conduction with thermal conductivity k and the second is the transport of energy due to mass diffusion, h_i being the enthalpy of component i.

A useful alternate form of the energy equation is obtained by introducing the component and mixture specific heats as well as the relation between h and h_i

$$c_{pi} = \partial h_i / \partial T, \quad c_p \equiv \Sigma c_{pi} \rho_i / \rho, \quad h \equiv \Sigma h_i \rho_i / \rho. \tag{2.5}$$

If these are used in equation (2.3) in order to introduce temperature derivatives, and (2.2) is used to eliminate the derivatives of ρ_i, the resulting form of the energy equation is

$$\rho c_p \left(\frac{\partial T}{\partial t} + v \frac{\partial T}{\partial y} \right) = \frac{\partial}{\partial y} \left(k \frac{\partial T}{\partial y} \right) - \Sigma \rho_i V_i c_{pi} \frac{\partial T}{\partial y} - \Sigma w_i h_i. \tag{2.6}$$

This form is the one suitable for use in frozen flow where $w_i = 0$, or for non-equilibrium flow, where w_i is a given function determined from the reaction equations.

To these equations must be added an equation of state, expressions for the diffusion fluxes $\rho_i V_i$ and thermal conductivity, and the boundary conditions. Assuming a catalytic wall, the latter are

$$y = 0: \quad v = 0, \quad T = T_w \text{ (given)}, \quad \rho = \rho_{\text{ATOMS}}. \tag{2.7a}$$

And

$$y \to \infty: \quad T \to T_e, \quad \rho_i \to \rho_{ie}. \tag{2.7b}$$

For case (1), that of a perfect unionized gas, there is only one component. The energy equation (2.6) with $w_i = V_i = 0$ and the continuity equation (2.1) are the equations to be solved. For case (2), a monatomic, ionized gas in thermodynamic equilibrium, there are three components—atoms, ions and electrons, but, because the ions and electrons diffuse in pairs by ambipolar diffusion, the mixture is basically binary.† Thus we need the equation (2.1) of over-all mass conservation, the energy equation, which we take in the form (2.3) for this case, and the equilibrium relation between the degree of ionization and the thermodynamic state variables, which in this case is the Saha equation. Finally, in case (3), for a monatomic, ionized gas with no gas-phase recombination (frozen), we need the equation (2.1) of over-all mass conservation, and the energy equation which we take in the form (2.6) with $w_i = 0$. The mixture is still binary, so we need again one relation for the degree of ionization, which in this case is an equation (2.2) for one-species mass conservation with $w_i = 0$. The one for the ions is convenient. For all these cases, suitable selections of the boundary conditions (2.7) are used.

The next section is devoted to specifying the thermodynamic and transport properties of the ionized argon mixture.

3. Thermodynamic and transport properties

Thermodynamic properties

For a mixture of atoms, singly-ionized ions and electrons, the thermodynamic properties are simply expressed. Only a single component concentration need be specified, and we will use the degree of ionization, α, defined by

$$\alpha \equiv n_I/(n_A+n_I), \quad n \equiv n_A+n_I+n_E = n_A+2n_I, \tag{3.1}$$

where the n's are particle concentrations per unit volume, and the subscripts A, I, E refer to atoms, ions and electrons. The mass densities ρ_i follow by introducing the masses m_i

$$\rho = (n_A+n_I)m_A, \quad \rho_I = n_I m_A = \alpha\rho, \quad \rho_E = n_E m_E = \rho_I m_E/m_A. \tag{3.2}$$

The partial pressures p_i are simply proportional to n_i so from (3.1) we find

$$p_A/p = (1-\alpha)/(1+\alpha), \quad p_I/p = p_E/p = \alpha/(1+\alpha), \tag{3.3}$$

while the gas law becomes

$$p = n\kappa T = \rho(1+\alpha)(\kappa/m_A)T, \tag{3.4}$$

with κ the Boltzmann constant.

The constant-pressure specific heat c_p of all particles is taken as $\frac{5}{2}\kappa$, and so, on a unit mass basis, we find

$$c_{pA} = c_{pI} = 5\kappa/2m_A, \quad c_{pE} = 5\kappa/2m_E, \quad c_p \equiv \Sigma c_{pi}(\rho_i/\rho) = c_{pA}(1+\alpha). \tag{3.5}$$

† This is an assumption which is valid provided the Debye distance is much smaller than the boundary-layer thickness, thus ensuring substantial charge neutrality. The sheath region at the wall, where such an assumption is no longer valid, is replaced by the boundary conditions for a fully catalytic wall discussed above.

The enthalpies follow from this with the introduction of h_I^0 as the ionization energy per unit mass of atoms:

$$\left.\begin{aligned} &h_A = c_{pA}T, \quad h_I = c_{pA}T + h_I^0, \quad h_E = c_{pE}T, \\ &h \equiv \Sigma h_i \rho_i/\rho = c_{pA}(1+\alpha)T + \alpha h_I^0 = c_p T + \alpha h_I^0. \end{aligned}\right\} \tag{3.6}$$

For the equilibrium case, we also need the Saha equation relating α to p and T. The form we shall use is

$$\alpha = \left[1 + p h_P^3 (\kappa T)^{-\frac{5}{2}} (2\pi m_E)^{-\frac{3}{2}} \frac{Q_{elA}}{Q_{elI} Q_{elE}} \exp(m_A h_I^0/\kappa T)\right]^{-\frac{1}{2}}, \tag{3.7}$$

where Q_{eli} is the electronic partition function of species i, and h_P is Planck's constant.

Transport properties

The transport properties needed for the calculation are the thermal conductivity of the mixture, k, and the diffusion fluxes $\rho_i V_i$. The diffusion terms in equations (2.4) and (2.6) can be simplified by using the zero-net-mass-diffusion-flux relation for the vector diffusion velocities $\mathbf{V}_i$,

$$\Sigma \rho_i \mathbf{V}_i = \rho_A \mathbf{V}_A + \rho_I \mathbf{V}_I = 0, \tag{3.8}$$

the ambipolar-diffusion condition $\mathbf{V}_I = \mathbf{V}_E$, and the expressions (3.2), (3.5), and (3.6) for the densities, specific heats, and enthalpies. The results are

$$\begin{aligned} \Sigma \rho_i V_i h_i &= \rho_A V_A h_A + \rho_I V_I h_I + \rho_E V_E h_E, \\ &= \rho_I V_I (h_I - h_A + h_E \rho_E/\rho_I), \\ &= \rho_I V_I (h_I^0 + c_{pA} T), \end{aligned} \tag{3.9a}$$

$$\begin{aligned} \Sigma \rho_i V_i c_{pi} &= \rho_I V_I (c_{pI} - c_{pA} + c_{pE} \rho_E/\rho_I), \\ &= \rho_I V_I c_{pA}, \end{aligned} \tag{3.9b}$$

Thus only the ion-diffusion flux must be specified, which is a consequence of the assumption of ambipolar diffusion.

The thermal conductivity of argon atoms has been computed by Amdur & Mason (1958) from 1500 to 15,000 °K using the results of beam experiments for argon atom collisions. These calculations can be represented by a power law

$$k_A = 5{\cdot}8 \times 10^{-7} T^{\frac{3}{4}} \text{ cal/cm sec °K}, \tag{3.10}$$

which also represents the lower temperature values of the National Bureau of Standards (1955). Although it is a few percent high between 1000 and 3000 °K, it gives the correct value at 300 as well as 15,000 °K, and we will use it as the thermal conductivity of atomic argon at all temperatures above 300 °K.

For a completely singly ionized gas the thermal conductivity k_S in the absence of any current flow is given by Spitzer (1956, pp. 87–88) as

$$k_S = 4{\cdot}4 \times 10^{-13} T^{\frac{5}{2}}/ln\Lambda_1 \text{ cal/cm sec °K}, \tag{3.11}$$

where Λ_1 is the ratio of the Debye distance to the impact parameter for 90° deflexion, given by Spitzer (1956, p. 72) as

$$\Lambda_1 \equiv \frac{3}{2}\left(\frac{\kappa T}{\pi n_E e^6}\right)^{\frac{1}{2}} = 1{\cdot}24 \times 10^4 T^{\frac{3}{2}}/n_E^{\frac{1}{2}}. \tag{3.12a}$$

Here ϵ is the electronic charge, T is in °K and n_E in electrons per cubic centimetre. For high electron density and low temperature, the Debye distance is smaller than the average distance between particles, $n_E^{-\frac{1}{3}}$, and should be replaced by the latter in determining Λ, giving

$$\Lambda_2 = 3\kappa T\epsilon^{-2}n_E^{-\frac{1}{3}} = 1800Tn_E^{-\frac{1}{3}}. \tag{3.12b}$$

The limit of validity of the use of Λ_2 is $\Lambda_2 \leqslant 12\pi$. For convenience in the calculations, the log term in equation (3.11) was taken as a combination of Λ_1 and Λ_2 in order to provide positive values of k_S which would still be correct in the limiting cases

$$k_S = \frac{4{\cdot}4\times 10^{-13}T^{\frac{5}{2}}}{\frac{1}{4}\ln(\Lambda_1^4+\Lambda_2^4+e^4)} \text{ cal/cm sec °K}. \tag{3.13}$$

For the mixture of atoms, ions, and electrons we will use the approximate mixture rule suggested by Fay (1964)

$$k = \sum_j \frac{x_j k_j}{\sum_i x_i G_{ji}}, \quad G_{ji} = \left(\frac{2m_i}{m_j+m_i}\right)^{\frac{1}{2}} \frac{Q_{ji}}{Q_{jj}}. \tag{3.14}$$

Here k_j and x_j are the thermal conductivity and mole fraction of the pure component j, and Q_{ji} is the effective hard-sphere cross-section for a collision pair j and i.

The binary diffusion coefficient D_{ji} and the thermal conductivity for the monatomic component j are related to the effective hard-sphere cross-sections by

$$D_{ji} = \frac{3}{16(n_j+n_i)Q_{ji}}\left[\frac{2\pi(m_j+m_i)\kappa T}{m_j m_i}\right]^{\frac{1}{2}}, \tag{3.15}$$

$$k_j = \frac{75\kappa}{64Q_{jj}}\left(\frac{\pi\kappa T}{m_j}\right)^{\frac{1}{2}}, \tag{3.16}$$

which are given, for example, by equations (10.22, 2) and (10.21, 1) of Chapman & Cowling (1960).

If the mixture rule (3.14) is to hold for a completely singly ionized plasma, then the electron and ion thermal conductivities should be chosen as

$$k_I(m_I/m_E)^{\frac{1}{2}} = k_E = (1+\sqrt{2})k_S, \tag{3.17}$$

since $Q_{EE} = Q_{II}$. Upon substituting these into the mixture rule, neglecting those G_{ji} having the factor $(m_E/m_A)^{\frac{1}{2}}$, and using equation (3.16) to relate Q_{EE} to Q_{AA}, we find for the mixture

$$k = k_S\left[1+\sqrt{2}\frac{m_E}{m_A}\frac{k_S}{k_A}\frac{Q_{AE}}{Q_{AA}}\frac{1-\alpha}{\alpha}\right]^{-1} + k_A\left[1+\frac{Q_{AI}}{Q_{AA}}\frac{\alpha}{1-\alpha}\right]^{-1}. \tag{3.18}$$

The ratio Q_{AE}/Q_{AA} is relatively unimportant in determining k because this term is small except when α is very small. Consequently, this ratio was chosen to be $1{\cdot}5\times 10^{-2}$ in accordance with the average values of these cross-sections in the temperature region of interest. To determine the ratio Q_{AI}/Q_{AA}, we find Q_{AA} from equation (3.16) applied to atoms with k_A from equation (3.10). For Q_{AI}, we use equation (3.15) for the binary diffusion coefficient D_{AI}, which can be

calculated from experimental data on the drift of ions through an atomic gas. According to kinetic theory, D_{AI} is related to the ratio of the drift velocity V_d and to the electric field E by (Chapman & Cowling 1960, p. 321)

$$D_{AI} = (V_d/E)\,(\kappa T_I/\epsilon). \tag{3.19}$$

The ion temperature T_I for these experiments may be taken to be that temperature for which the mean thermal speed equals the drift velocity

$$8\kappa T_I/\pi m_I = V_d^2. \tag{3.20}$$

Using the data from experiments by Hornbeck (1951), Q_{AI} for argon was calculated from equations (3.15), (3.19), and (3.20). When combined with Q_{AA} this yields

$$Q_{AI}/Q_{AA} = 1{\cdot}44T^{0{\cdot}16}, \tag{3.21}$$

with T in °K.

We now have specified all the quantities necessary to write the thermal conductivity of the mixture k from equation (3.18), as a function of temperature and fraction ionized, and the physical constants of the atoms and electron.

Turning to the mass-flux of ions due to ambipolar diffusion, we consider a two-component mixture of atoms and ion-electron pairs. The momentum equation for diffusing atoms may be written in the form:

$$-\nabla p_A = \left[\frac{m_I m_A}{m_I + m_A}(\mathbf{V}_A - \mathbf{V}_I)\right][\tfrac{4}{3}n_I n_A C_{AI} Q_{AI}], \tag{3.22}$$

in which $C_{AI} = [8(m_I+m_A)\kappa T/\pi m_I m_A]^{\frac{1}{2}}$ is the mean relative velocity of the colliding atoms and ions. The first factor is brackets is the momentum loss per atom-ion collision and the second is the total collision frequency, which is chosen so that the usual diffusion equation for a binary mixture (equation (8.41, 3) of Chapman & Cowling 1960) is obtained when equation (3.15) is used to eliminate Q_{AI} in equation (3.22). The statement is that the momentum gain due to pressure gradient is balanced by the momentum loss due to collisions with counter-diffusing ions. The electrons contribute nothing to this momentum balance because of their small mass.

If Q_{AI} is eliminated from equation (3.22) using equation (3.15), $\mathbf{V}_A$ is eliminated by means of the zero-net-mass-diffusion-flux condition (3.8), and the number densities are replaced by α from equation (3.1), we find

$$\rho_I \mathbf{V}_I = m_A D_{AI}(\kappa T)^{-1}\nabla p_A.$$

For simple diffusion the total pressure is constant, so we can differentiate the ratio p_A/p from equation (3.3) to find ∇p_A. Use of the gas law then yields

$$\rho_I \mathbf{V}_I = -D_{am}\rho\nabla\alpha, \quad D_{am} \equiv 2(1+\alpha)^{-1}D_{AI}. \tag{3.23}$$

This defines the ambipolar diffusion coefficient D_{am} in terms of the atom-ion diffusion coefficient D_{AI} of equation (3.19). D_{am} is seen to be twice D_{AI} for small degrees of ionization, a familiar result. For high degrees of ionization, D_{am} approaches D_{AI}.

For use in boundary-layer theory, D_{am} is replaced by the ratio of particle

diffusivity to thermal diffusivity, called the Lewis number. A useful definition in the present case is based on D_{am}, the atomic thermal conductivity and the constant-pressure specific heat per unit volume of the mixture:

$$L_A \equiv \frac{D_{am}(\rho c_p)}{k_A} = \frac{2D_{AI}}{1+\alpha}\frac{n_A+n_I}{k_A}\frac{5\kappa}{2}(1+\alpha) = \frac{8}{5}\frac{Q_{AA}}{Q_{AI}}. \tag{3.24}$$

The second step comes from equations (3.23), (3.2) and (3.5), while the last comes from eliminating D_{AI}/k_A from (3.15) and (3.16). By using the experimentally determined cross-section ratio from equation (3.21) we find

$$L_A = 1{\cdot}11T^{-0{\cdot}16} = 0{\cdot}255(T/10^4)^{-0{\cdot}16}, \tag{3.25}$$

where T is in °K.

Finally, in terms of L_A from (3.24), the ion-diffusion mass flux, equation (3.23), becomes

$$\rho_I V_I = -(k_A L_A/c_p)\,\partial\alpha/\partial y, \tag{3.26}$$

where we have only written the y component, since that is all we need in the diffusion terms (3.9) in our equations.

Now that the thermodynamic and transport properties are specified in terms of T and α, we may proceed to the solution of the boundary-layer equations.

4. Transformed equations

The partial differential equations and boundary conditions of § 2, together with the thermodynamic and transport properties of § 3, define the problem of calculating heat transfer to the wall in a hot argon plasma. For the unionized, equilibrium and frozen cases considered here, the problem has a similarity solution† in which the dependent variables are only a function of a single independent variable, which may be defined as

$$\eta \equiv \left(\frac{c_{p0}}{2t\rho_0 k_0}\right)^{\frac{1}{2}} \int_0^y \rho\, dy. \tag{4.1}$$

The quantities denoted by the subscript 0 are reference quantities which may be evaluated at any arbitrary but constant state. In the computations we will assume the reference state to be that of the undisturbed plasma external to the boundary layer. A set of normalized dependent variables are also defined by

$$\theta(\eta) \equiv T/T_e, \quad s(\eta) \equiv \alpha/\alpha_e. \tag{4.2}$$

With this transformation the over-all-mass-conservation equation (2.1) may be solved for ρv, and the convective derivative operator becomes

$$\rho\frac{\partial}{\partial t} + \rho v\frac{\partial}{\partial y} = \frac{-\rho\eta}{2t}\frac{d}{d\eta}. \tag{4.3}$$

† We assume conditions behind the shock wave but outside the boundary layer are constant in time and space, although this is not completely consistent with the effect of the boundary-layer displacement thickness which increases (negatively) with time. However, this approximation is the usual one always employed in first order boundary-layer theory.

Then we may transform the energy equation (2.3) and the energy flux (2.4), using equations (3.9a) and (3.26) for the diffusion term. The result is

$$\frac{d}{d\eta}\left[\frac{k\rho}{k_0\rho_0}\frac{d\theta}{d\eta}+\frac{k_A\rho}{k_0\rho_0}\frac{c_{pA}}{c_p}L_A\left(\theta+\frac{h_I^0}{c_{pA}T_e}\right)\frac{d\alpha}{d\eta}\right]+\frac{c_{pA}}{c_{p0}}\frac{d}{d\eta}\left[\frac{h}{c_{pA}T_e}\right]=0, \tag{4.4}$$

$$-q_y=\left[\frac{c_{p0}k_0\rho_0}{2t}\right]^{\frac{1}{2}}T_e\left[\frac{k\rho}{k_0\rho_0}\frac{d\theta}{d\eta}+\frac{k_A\rho}{k_0\rho_0}\frac{c_{pA}}{c_p}L_A\left(\theta+\frac{h_I^0}{c_{pA}T_e}\right)\frac{d\alpha}{d\eta}\right]. \tag{4.5}$$

For equilibrium, α is related to θ through the Saha equation (3.7) so $d\alpha/d\eta$ can be related to $d\theta/d\eta$. Furthermore, h is also related to θ and α by equation (3.6). When these are inserted in equations (4.4) and (4.5) we find

$$\frac{d}{d\eta}\left[\frac{k\rho}{k_0\rho_0}\frac{d\theta}{d\eta}\left(1+L_A\frac{k_A}{k}S\right)\right]+\eta\frac{c_p}{c_{p0}}(1+S)\frac{d\theta}{d\eta}=0, \tag{4.6}$$

$$-q_y=\left[\frac{c_{p0}k_0\rho_0}{2t}\right]^{\frac{1}{2}}T_e\left[\frac{k\rho}{k_0\rho_0}\frac{d\theta}{d\eta}\left(1+L_A\frac{k_A}{k}S\right)\right], \tag{4.7}$$

where

$$S\equiv\frac{\theta+h_I^0/c_{pA}T_e}{c_p/c_{pA}}\frac{d\alpha}{d\theta}=\frac{5}{4}\frac{a(1-\alpha^2)}{\theta^2c_p/c_{pA}}(\theta+h_I^0/c_{pA}T_e)^2. \tag{4.8}$$

In the case of thermodynamic equilibrium, θ is the only variable, so only equation (4.6) need be solved, and then equation (4.7) gives the heat-transfer rate when evaluated at the wall $\eta=0$. The boundary conditions on θ are given in equations (2.7).

For the frozen case, the transformation is applied to equations (2.2) and (2.6) with $w_i=0$. Equation (2.2) is written for ions, with (3.26) used for the diffusion mass flux. In equation (2.6) we use (3.9b) and (3.26) for the diffusion term. We find

$$\frac{d}{d\eta}\left[\frac{k_A\rho/c_p}{k_0\rho_0/c_{p0}}L_A\frac{ds}{d\eta}\right]+\eta\frac{ds}{d\eta}=0, \tag{4.9}$$

$$\frac{d}{d\eta}\left(\frac{k\rho}{k_0\rho_0}\frac{d\theta}{d\eta}\right)+\left[\eta\frac{c_p}{c_{p0}}+\frac{k_A\rho/c_p}{k_0\rho_0/c_{p0}}L_A\frac{c_{pA}}{c_{p0}}\alpha_e\frac{ds}{d\eta}\right]\frac{d\theta}{d\eta}=0. \tag{4.10}$$

The corresponding heat-flux expression is just equation (4.5). In this case both θ and s are unknown, and both equations (4.9) and (4.10) must be solved, subject to the boundary conditions given in equations (2.7), which include the catalytic wall condition $s=0$ at $n=0$.

The third case of interest, the unionized perfect gas, is a simple limiting case of either equation (4.6) or (4.10) with $\alpha=0$, and c_p constant. This energy equation is

$$\frac{d}{d\eta}\left(\frac{k_A\rho}{k_0\rho_0}\frac{d\theta}{d\eta}\right)+\eta\frac{d\theta}{d\eta}=0, \tag{4.11}$$

also subject to the θ boundary conditions of equations (2.7). This equation can, of course, be integrated on a machine like the others. However, if only the wall-heat-transfer rate is desired, it is simple enough to be attacked analytically, since k_A is the power function of T indicated in equation (3.10). An integral method has been applied when

$$k_A\propto T^\nu,\quad \rho\propto T^{-1}, \tag{4.12}$$

and an accurate analytical formula for wall-heat-transfer rate has been found (Jepson 1961, Kemp 1964). The result is

$$q_{yw} \equiv (-q_y)_{\eta=0} = 1{\cdot}13\left[\frac{\rho_e k_{Ae} c_{pe}}{2t}\right]^{\frac{1}{2}} T_e\left[\frac{1-\theta_w^{\nu}}{\nu} - \frac{1-\theta_w^{\nu+1}}{\nu+1}\right]^{\frac{1}{2}}. \tag{4.13}$$

This formula agrees with numerical integrations of equation (4.11) under the conditions (4.12) within $\pm 3\,\%$ for $0{\cdot}5 \leqslant \nu \leqslant 2{\cdot}5$ and $0 \leqslant \theta_w \leqslant 1$. In the present case of interest, $\nu = \frac{3}{4}$ according to equation (3.10).

For the solution of the equilibrium and frozen cases, numerical integration on a digital computer was used. The formulation of the equations for the computer is described in appendix B of Fay & Kemp (1963).

5. Calculations, results and discussion

Calculations have been made for argon for cases corresponding to conditions on the end wall of a shock tube. The initial pressure p_i in the tube was 1 mm Hg, and the incident shock speed varied from 3 to 6 mm/μsec. In order to get the input data, it was necessary to calculate conditions behind a reflected shock in argon. Such calculations are straightforward for argon considered as a perfect gas with no ionization, and the necessary input data are given in table 1, with U_s the incident shock speed. Also given is $q\sqrt{t}$ calculated from equation (4.13), with k_{Ae} and ν from equation (3.10).

U_s (mm/μsec)	p/p_i	T_e (°K)	$q\sqrt{t}$ (W/cm^2)(sec)$^{\frac{1}{2}}$
3	630	19,500	2·71
4	1150	34,100	6·00
5	1810	54,100	11·4
6	2610	77,900	18·8

TABLE 1. Heat transfer calculations for non-ionized argon ($p_i = 1$ mm Hg).

For argon which ionizes behind the incident shock, a more complicated condition ensues. A schematic distance-time diagram is shown in figure 1. Behind the incident shock there is a region where the gas has not yet had time to ionize, region 2F. This is followed after a time interval τ_2 by a rapid ionization process, denoted by a dotted line, followed by a region 2E where the argon is in equilibrium behind the incident shock. The ionization process is quite fast in argon, and as a first approximation may be considered to take place in a sharp front. When the incident shock arrives at the end-wall, it reflects back into the as yet unionized argon, making a region 2F 4F in which the argon is still unionized. In this region the unionized perfect gas model is applicable. After a time τ_4, which is less than τ_2 because of the higher temperature and pressure, this gas ionizes, giving a region 2F 4E′. This ionization process sends out expansion waves, because of its large increase in density, and reduces the speed of the reflected shock. Further interactions occur when the reflected shock meets the ionization front behind the incident shock.

The calculation of conditions at the end-wall in region 2F 4E′, and later, is obviously very difficult. In addition, this discussion shows that the external

conditions for our boundary-layer problem are not constant, so that a local-similarity analysis cannot be exactly applicable except in the perfect-gas region, 2F 4F. However, we have made calculations in the frozen and equilibrium cases in order to compare them with experimental results available that go from the

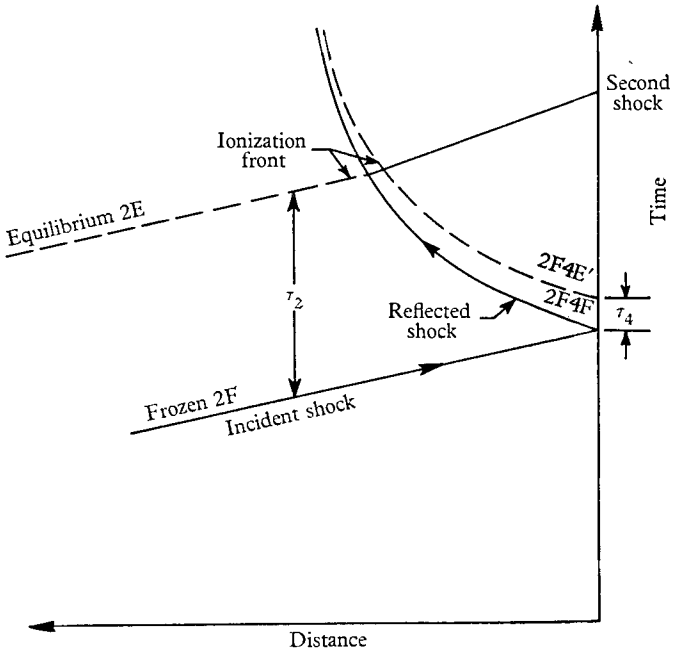

FIGURE 1. Distance-time diagram for the flow at the end-wall.

2F 4F region into the 2F 4E′ region. These heat-transfer measurements are described by Camac & Feinberg (1965). The conditions in region 2F 4E′ used as boundary conditions were obtained by a method described by Camac & Teare (1964), which approximated the distance–time diagram of figure 1 by a conical-flow picture. The resulting external conditions are given in table 2, together with the result of heat-transfer calculations based on these conditions.

The values of $q\sqrt{t}$ given in table 1 for unionized argon and table 2 for region 2F 4E′ are plotted against shock speed in figure 2. Also presented there are the experimental measurements of Camac & Feinberg (1965). These measurements represent heat-transfer rates in both the 2F 4F and 2F 4E′ regions, since the experimental rates did not change during the ionization process.

The agreement of the unionized-perfect-gas calculations with the experimental rates is striking. The only unknown in this calculation is the thermal conductivity of atomic argon k_A. This was taken as equation (3.10), which was based on the calculations of Amdur & Mason (1958) up to 15,000 °K, and then used up to 78,000 °K. The remarkable agreement with experiment can be interpreted as confirming this $T^{\frac{1}{2}}$ dependence of k_A up to the temperature limit of the experiments, which is 75,000 °K.

Comparison of the frozen and equilibrium results with experiment in figure 2 shows the frozen to be low by up to 40 % and the equilibrium to be low by up

U_e (mm/μsec)	p (atm.)	T_e (°K)	α_e	$q\sqrt{t}$ (W/cm^2) (sec)$^{\frac{1}{2}}$ Equil.	Frozen
		2F 4E′			
3	0·714	11,300	0·0818	2·48	3·00
4	1·18	12,900	0·206	4·94	4·26
5	1·78	14,400	0·366	8·42	7·00
6	2·52	15,800	0·559	13·1	10·6
		2F 4E			
3	0·725	11,100	0·070	2·34	2·17
4	1·22	12,700	0·175	4·62	3·90
5	1·84	14,100	0·315	7·94	6·33
6	2·62	15,500	0·485	12·56	9·60
		2E 4E			
3	0·790	11,200	0·072	2·49	2·30
4	2·04	13,400	0·217	6·73	5·66
5	4·35	15,400	0·385	14·5	11·3
6	7·90	17,500	0·600	26·5	20·0

TABLE 2. Heat transfer calculations for ionized argon (p_i = 1 mm Hg).

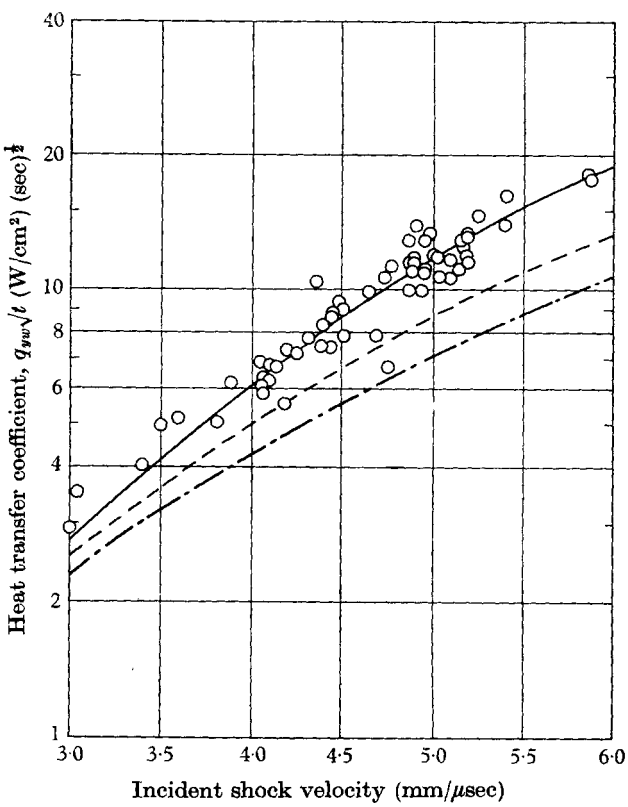

FIGURE 2. Heat transfer rate to end-wall in argon with initial pressure p_i = 1 mm Hg, for non-ionized case and for region 2F 4E′. ○, experimental (Camac & Feinberg 1965); ——, $\gamma = \frac{5}{3}$ in 2F 4F; – – –, equilibrium boundary layer in 2F 4E′; —·—, frozen boundary layer in 2F 4E′.

to 30 %. It is apparent that these calculations are not as precise descriptions of the physical situation as one would like.

The possible sources of the discrepancy on the experimental side are discussed by Camac & Feinberg (1965). On the theoretical side they include, first, the use of only frozen and equilibrium calculations with the local similarity assumption during a period when the external conditions are changing from frozen to

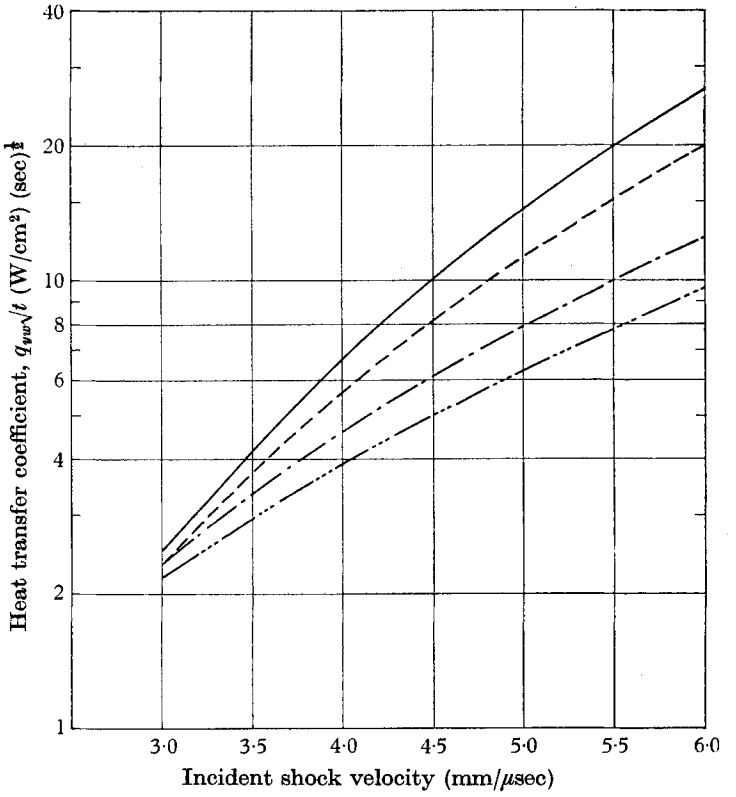

FIGURE 3. Heat-transfer rate to end-wall in argon with initial pressure p_i = 1 mm Hg, for regions 2F 4E and 2E 4E, where the reflected shock is a simple equilibrium transition but the incident shock is a frozen or equilibrium transition, respectively. ——, Equilibrium boundary layer in 2E 4E; – – –, frozen boundary layer in 2E 4E; —·—, equilibrium boundary layer in 2F 4E; —···—, frozen boundary layer in 2F 4E.

equilibrium. Secondly, the state of the gas at the edge of the boundary layer was obtained by an approximate method which may introduce some error. Thirdly, the theory considers only a single temperature, i.e. the temperature of the electrons is taken equal to that of the atoms and ions. While the ions and atoms reach temperature equilibrium in one collision, it takes 10^5 collisions for the electrons to equilibrate with the heavy particles. Also, there is a plasma sheath at the wall, which tends to reflect electrons and insulate them from the wall and its temperature level. Thus, a more accurate theoretical model should consider different electron and heavy temperatures, with the appropriate energy exchange due to collisions, the effects of the wall plasma sheath, and possible gas-phase electron-ion recombination. Such a model has been formulated (Camac & Kemp

1963) and is being studied for comparison with the results of the present investigation. This model shows that, when the temperatures are equal, the plasma sheath has a negligible effect on heat transfer, thus verifying the initial assumption made in the present investigation.

Considering all these possible sources of error for the present simple theoretical model, it is felt that the frozen and equilibrium calculations and the measurements show a substantial amount of agreement.

For comparison purposes, calculations have also been made using as outer boundary conditions the conditions at the end-wall when the incident shock is a frozen transition but the reflected shock is a simple equilibrium transition (2F 4E) and when both shocks are simple equilibrium transitions (2E 4E). The frozen- and equilibrium-boundary-layer heat-transfer for each of these two external conditions is shown in figure 3, and tabulated in table 2 as 2F 4E and 2E 4E. The substantial spread in the results indicates the importance of the chemical behaviour not only in the boundary layer but also in the inviscid flow. Comparison with figure 2 shows that the 2F 4E′ curves are only slightly above the 2F 4E curves, and that the non-ionized argon curve lies very close to the 2E 4E frozen-boundary-layer curve. The 2E 4E equilibrium-boundary-layer curve is above all the experimental points except a few below $U_s = 4\,\mathrm{mm}/\mu\mathrm{sec}$.

This research was sponsored by the Ballistic Systems Division of the Air Force Systems Command under contract no. AF 04(694)-33. Mr William Nelson performed the machine calculations. Dr Morton Camac contributed to many fruitful discussions.

REFERENCES

AMDUR, I. & MASON, E. A. 1958 *Phys. Fluids*, **1**, 370.

CAMAC, M. & FEINBERG, R. M. 1965 *J. Fluid Mech.* **21**, 673.

CAMAC, M. & KEMP, N. H. 1963 *Amer. Inst. Aero. Astro. Paper* no. 63–460.

CAMAC, M. & TEARE, J. D. 1964 *Avco-Everett Res. Lab. Res. Rep.* no. 183.

CHAPMAN, S. & COWLING, T. G. 1960 *The Mathematical Theory of Non-Uniform Gases*, 2nd Ed. Cambridge University Press.

EDWARDS, D. K. & TELLEP, D. M. 1961 *ARS J.* **31**, 652.

FAY, J. A. 1964 *The High Temperature Aspects of Hypersonic Flow*, p. 583 (ed. W. C. Nelson). London: Pergamon Press.

FAY, J. A. & KEMP, N. H. 1963 *Avco-Everett Res. Lab. Res. Rep.* no. 166.

HANSEN, C. F., EARLY, R. A., ALZOFON, F. E. & WITTENBORN, F. C. 1959 *Nat. Aero. Space Admin. Tech. Rep.* no. R-27. See also *ARS J.* **30**, 942 (1960).

HORNBECK, J. 1951 *Phys. Rev.* **84**, 615.

JEPSON, B. M. 1961 *Dept. Mech. Eng. Magnetogasdynamics Lab., M.I.T., Cambridge, Rep.* no. 61–7.

KEMP, N. H. 1964 *Dept. Mech. Eng. Fluid Mech. Lab., M.I.T., Cambridge, Pub.* no. 64–6.

LAUVER, M. R. 1964 *Phys. Fluids*, **7**, 611.

NATIONAL BUREAU OF STANDARDS 1955 *Government Printing Office, Wash., Circular* no. 564.

PENG, T. C. & AHTYE, W. F. 1961 *Nat. Aero. Space Admin. Tech. Note* no. D-687.

SMILEY, E. F. 1957 Ph.D. Thesis, Catholic University of America.

SPITZER, L. 1956 *Physics of Fully Ionized Gases*, New York: Interscience Publishers, Inc.

THOMSON, T. A. 1960 *Australian Defence Scientific Services Aero. Res. Lab. Aero. Note* no. 186.